IEEE Access
Multidisciplinary | Rapid Review | Open Access Journal

Received January 21, 2018, accepted March 16, 2018, date of publication April 3, 2018, date of current version May 24, 2018.

Digital Object Identifier 10.1109/ACCESS.2018.2819163

A Low Profile UWB Antenna for WBAN Applications

DEQIANG YANG[1], JIANZHONG HU[1], AND SIHAO LIU[2]
[1]School of Electronic Engineering, University of Electronic Science and Technology of China, Chengdu 611731, China
[2]School of Materials and Energy, University of Electronic Science and Technology of China, Chengdu 611731, China

Corresponding author: Sihao Liu (s_h_liu@163.com)

ABSTRACT In this paper, we propose a low-profile ultra-wideband (UWB) antenna for wireless body area networks. The proposed antenna is low-weight and easy to produce by printed circuit board manufacturing. Optimized shape of the radiation patch and shorted top-loading patches are introduced to broaden the bandwidth and reduce the profile of the antenna. The height of the antenna is $0.05\lambda_0$, where λ_0 is the free-space wavelength at the lowest operating frequency. The simulated and measured results show that an enhanced impedance bandwidth of about 162% in the range of 2.5 to 24 GHz ($S_{11} < -10$ dB) is achieved. Besides, the influence of the human body to the proposed antenna is minimal. The time-domain behavior of the low-profile UWB antenna is tested, and the results show a satisfactory performance in transmitting and receiving pulse signals.

INDEX TERMS Low profile, ultrawideband antenna, WBAN.

I. INTRODUCTION

In February 2002, the Federal Communications Commission (FCC) assigned the frequencies of 3.1 GHz to 10.6 GHz in the UWB spectrum for commercial use. Applications based on UWB technology have achieved considerable development due to their appealing characteristics, such as high-speed transmission rate and high multi-pathway resolution; WBANs are among the most attractive applications [1]. The antenna plays a crucial role in ensuring the operation of a WBAN system. As the antenna of a WBAN can be placed on a human body, the influence of the wearer on the transient characteristics should be considered in the antenna design [2]. The electric field parallel to the human body generates a polarization current on the human body. As a result, the gain and efficiency of a UWB antenna are degradative. To overcome this problem, the UWB antenna used for a WBAN should have vertical polarization. Meanwhile, to communicate with other devices, a monopole-like radiation characteristic is required.

Various UWB antennas have been proposed to achieve the low-profile character [3]–[12]. In [5], a wideband antenna composed of a conducting body of revolution and a shorted parasitic ring is proposed. This antenna is fed by the inner conductor of a coaxial feed line and can be considered as a top-loading monopole antenna. Monocone is another kind for omnidirectional UWB antenna. Compared with the top-loading monopole antenna proposed in [5], the monocone antenna has a broader bandwidth because it exemplifies a travelling wave structure. In [6], a low-profile UWB antenna designed to operate at 50 MHz up to 2 GHz is proposed. A monocone antenna with a top-loading circular patch is presented in [7]. In this work, to obtain low profile characteristic, four shorting probes are utilized to connect the top-loading patch and the ground plane. Chahat presented a reduced-size printed antenna for the UWB band. By extending the slot length the antenna, the height of the antenna is reduced to 10 mm [8]. In [9], a broadband, vertically polarized, and omnidirectional monocone antenna with a height of only $\lambda_0/14.7$ is presented. [10] proposes a low-profile UWB monocone antenna with cross-plate top loading and a relative height of 0.08 λ_0. In [11], an ultra-wideband antenna that operates in TM_{41} resonance mode is presented. This antenna has a low-profile structure with omnidirectional radiation characteristics. In [12], a stacked patch antenna with a height of 0.08 λ_0 is designed for UWB applications. However, the above-mentioned monocone antennas have a heavyweight and require particular fabrication for the cone.

The present study proposes a low-profile UWB antenna. In our design, to overcome the drawbacks of the monocone antenna, we project the monocone antenna onto a 2D plane, which enables the proposed antenna to be easily printed on a PCB. The antenna can integrate the unique characteristics of the monocone (e.g., broadband and monopole radiation) and

the benefits of the printed antenna (e.g., lightweight and easy fabrication). To achieve the low-profile character, a shorted circular ring patch and an optimized shape are applied. Both of the frequency-domain and time domain characteristics are simulated and measured. Results of S-parameters, radiation pattern, gain, MRG(mean realized gain), group delay and system-fidelity-factor are presented. The time domain results indicate that the proposed antenna has a satisfactory time domain response.

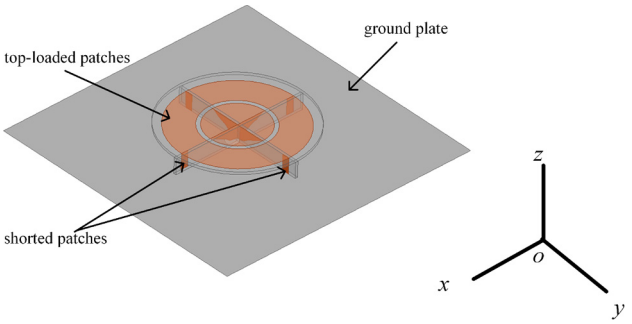

FIGURE 1. Geometry of the proposed UWB antenna.

II. ANTENNA DESIGN

Based on the monocone antenna, the proposed antenna uses a traveling wave structure to replace the common coaxial feed line. This structure can extend the low-end frequency limitation, therefore reduce the antenna profile. Besides, in our design, we project the traditional monocone antenna onto a 2D plane to overcome its drawbacks. Fig. 1 shows the geometry of the proposed UWB antenna, which consists of three substrates and a metalized ground plate. Specifically, the antenna has, from top to bottom, a horizontal substrate, two orthogonally placed vertical substrates, and a metalized ground plate. All the substrates are made of the standard FR-4 material with a thickness of 1 mm; the metalized ground plate is copper and 80 mm × 80 mm in size. Fig. 2 shows the bottom of the horizontal substrate. On the bottom surface of the horizontal substrate are a circular patch and a ring patch, which act as a capacitive load. The radius of the circular patch is R. The inside and outside radii of the ring patch are r_1 and r_2, respectively. The width of the gap between the ring patch and the circular patch is g. To explain the effect of the top-loading patches, we compare the different simulation results when this segment exists or not, as shown in Fig. 3. It can be observed that by adding top-loading patches to the proposed antenna, a low frequency resonance is obtained at 3 GHz. This second resonance significantly increases the bandwidth and reduces the profile of the antenna.

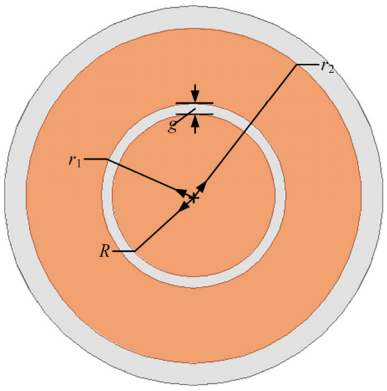

FIGURE 2. Bottom side of the horizontal substrate.

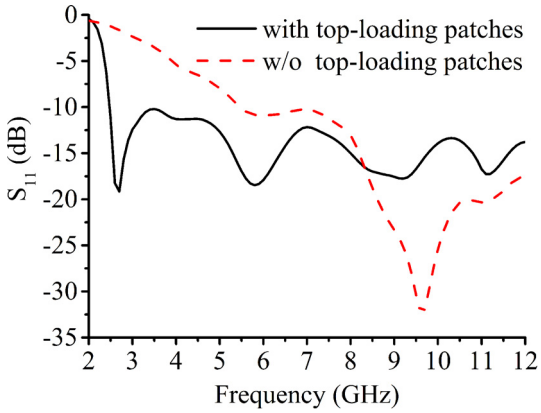

FIGURE 3. Simulated S_{11} characteristics of the proposed antenna with and without the top-loading patches.

To increase the symmetry, we use two orthogonally placed vertical substrates, forming a cross structure between the horizontal substrate and the ground plate. Fig. 4 shows the side view of the vertical rectangular substrate. A radiation patch and two shorted patches are printed on the vertical substrate. The shorted patches connect the ring patch to the ground plate.

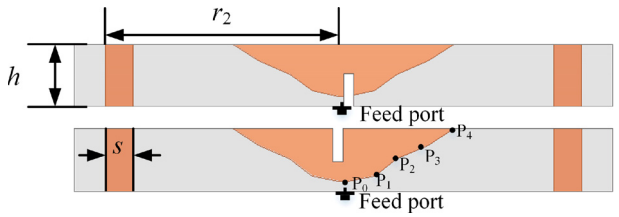

FIGURE 4. Side view of the vertical rectangular substrate.

A random walk scheme is used to optimize the line profile of the radiation patch. In particular, the line profile is made up of polyline that is characterized by the coordinates of the vertices. The $P_j(x_j, z_j)$ is the coordinates of the P_j in Fig. 4. Fig. 5 shows the schematic diagram of the optimized line profile, the parameters of which are presented in Table I. Some key optimized parameters of the antenna are: $R = 11$ mm, $r_1 = 12$ mm, $r_2 = 23$ mm, $g = 1$ mm, $h = 6$ mm, and $s = 2.7$ mm.

To better evaluate the performance of the proposed antenna, Fig. 6 presents the simulated surface current distributions of the proposed antenna at 3.1 GHz, 6.5 GHz,

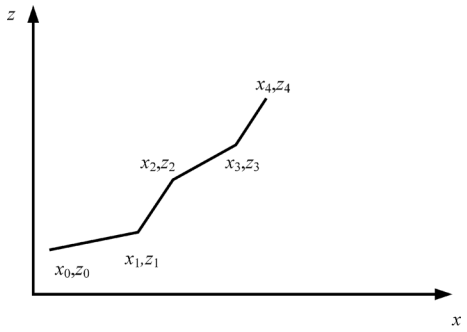

FIGURE 5. Schematic diagram of optimized shape.

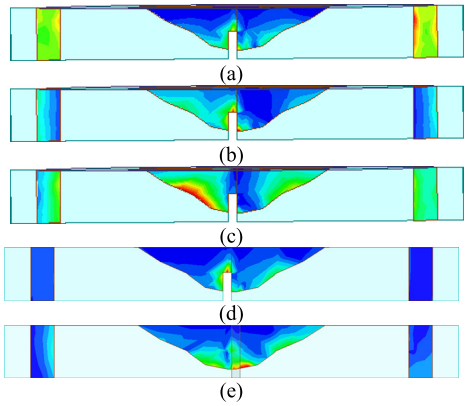

FIGURE 6. Simulated surface current distributions of proposed antenna at (a) 3.1 GHz, (b) 6.5 GHz, (c) 10 GHz, (d) 15 GHz, and (e) 20 GHz.

TABLE 1. Parameters of the shape.

j	0	1	2	3	4
x_j(mm)	0	3	5.17	8.17	10.64
z_j(mm)	1	1.5	3.1	4.4	6

10 GHz, 15 GHz, and 20 GHz. The results show that the currents are concentrated on the shorted patches at low frequency. As the frequency increases, the currents on the shorted patches become relatively weak. At high frequency, the currents are concentrated near the feed. This phenomenon indicates that changing the width of the shorted patches can significantly affect the low resonant frequency. Fig. 7 presents the simulated S_{11} for five different widths of s. The low resonant frequency also changes with varying values of s. This phenomenon provides an opportunity to formulate an effective way to adjust the lowest operating frequency.

III. RESULTS AND ANALYSES

A working prototype of the proposed low-profile UWB antenna is fabricated, as shown in Fig. 8.

A. Frequency-Domain Behavior

Figure 9 presents the measured and simulated magnitudes of the S_{11} of the low-profile UWB antenna. To study the effect of the human body, we have measured the fabricated antenna

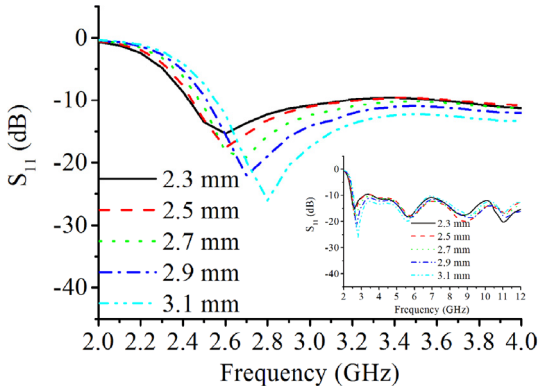

FIGURE 7. Simulated S_{11} for five different widths of s. Inset: full UWB band to illustrate that higher frequencies in the band remain unaffected.

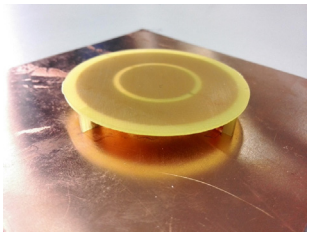

FIGURE 8. Photograph of the manufactured antenna.

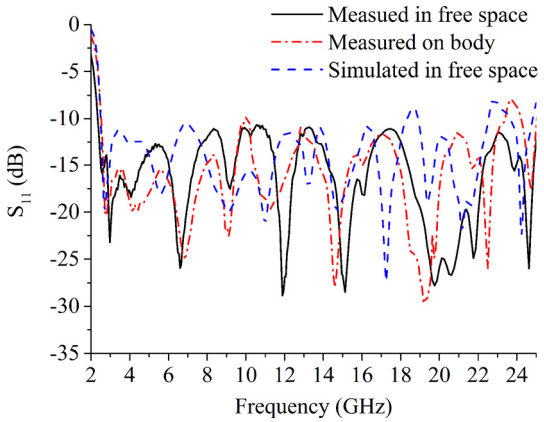

FIGURE 9. Measured and simulated S_{11}.

in free space and on a human body, respectively. As shown in the figure, the impedance bandwidth of the low-profile UWB antenna reaches 162% at $S_{11} < -10$ dB in the range of 2.5 GHz to 24 GHz, which is wide enough to cover the entire UWB band.

The comparison of the results measured in free space with those measured on the human body indicates that the human body does not significantly influence the behavior of the proposed low-profile UWB antenna. The slight variation between the measured and the simulated results are attributed to the manufacturing errors and the experimental environment.

To determine the radiation performance of the low-profile UWB antenna, we have simulated and measured the normalized far-field radiation patterns of the proposed antenna.

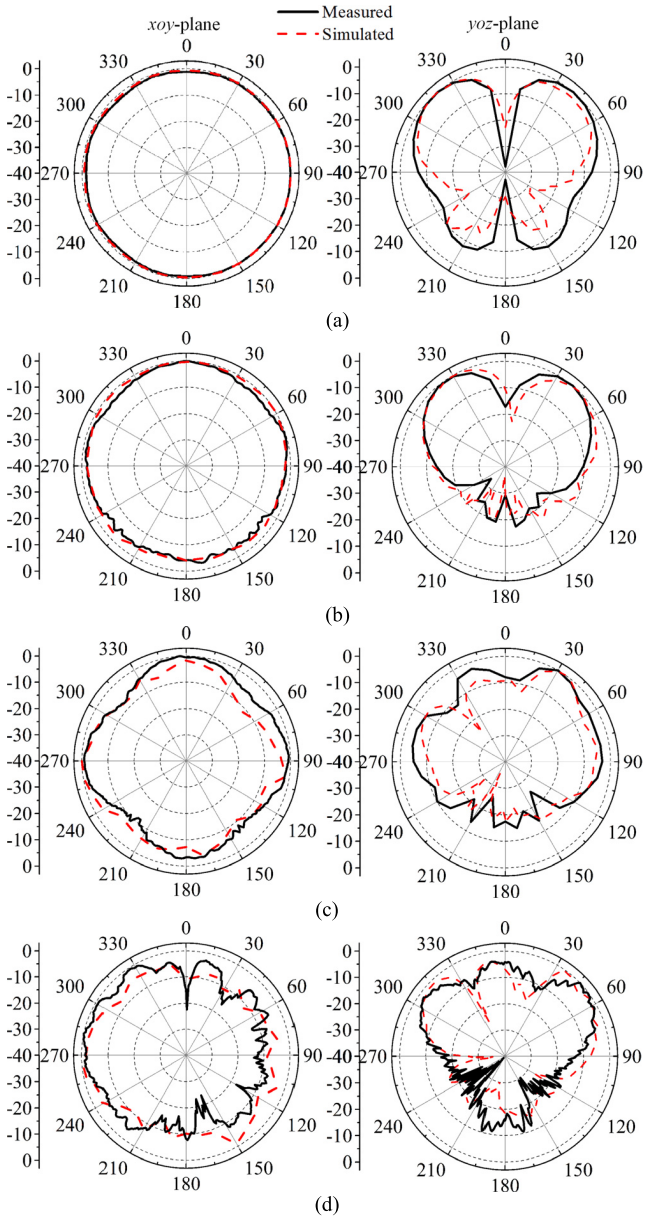

FIGURE 10. Measured radiation patterns for the (a) 3 GHz, (b) 6 Ghz, (c) 9 GHz, and (d) 12 GHz.

Fig. 10 shows the simulated and measured normalized far-field radiation patterns in the *xoy*-plane and *yoz*-plane at 3 GHz, 6 GHz, 9 GHz, and 12 GHz, respectively. The gain roundness of the *xoy*-plane at the selected frequencies are 1.5 dB, 4.3 dB, 10.3 dB, and 21 dB, respectively. Based on the measured results, the proposed antenna has omnidirectional radiation patterns in the *xoy*-plane in most of the UWB band (3.1-10.6 GHz). Because of the high-order mode resonance, the radiation patterns rise and fall at high frequencies. These radiation properties are acceptable over the entire UWB band. Fig. 11 illustrates the simulated and measured maximum realized gain of the low-profile UWB antenna, which ranges from 3 dBi to 10 dBi across the frequency band.

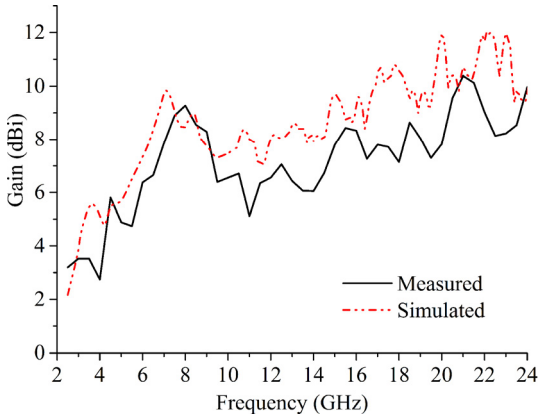

FIGURE 11. Simulated and measured maximum realized gain of the low profile UWB antenna.

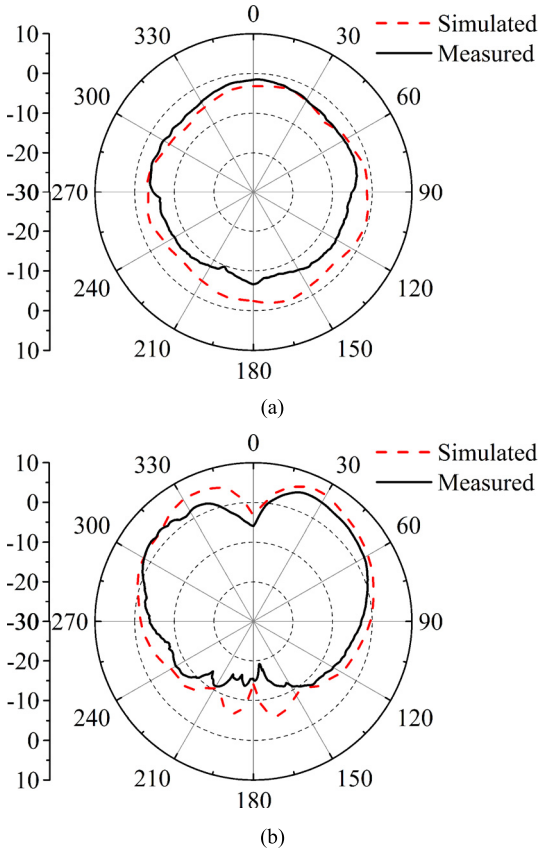

FIGURE 12. Simulated and measured MRG for the (a) xoy plane, and (b) yoz plane.

B. TIME-DOMAIN BEHAVIOR

Time-domain characterization of impulse radio UWB antennas is as important as its frequency-domain characterization.

The MRG is a synthetic, but intrinsic, indicator for the characteristic of the radiation properties of a UWB antenna over wide frequency [13]-[14]. The MRG is defined as

$$MRG(\hat{r}) = \frac{1}{BW_i} \int_{f_1}^{f_2} G_r(\hat{r}, f) df \quad (1)$$

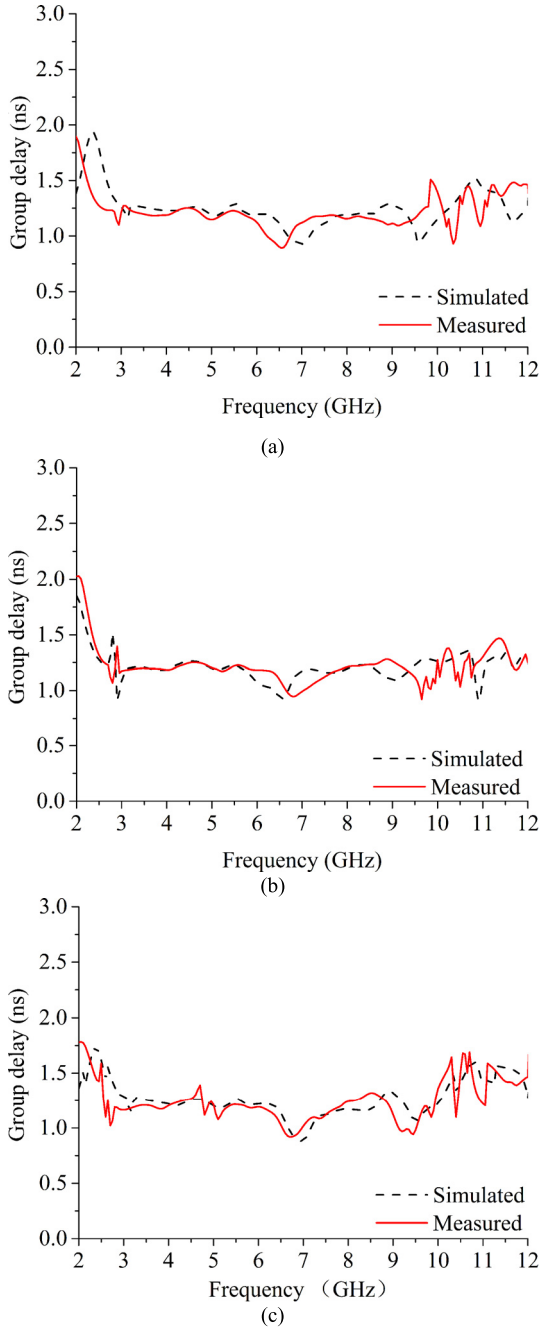

FIGURE 13. Group delay of the antenna system of theta = 90◦ at (a) φ =0◦, (b) φ = 15◦, and (c) φ =30◦.

The simulated and measured MRG ranging from 3.1 GHz to 10.6 GHz are shown in Fig. 12. It can be observed that the proposed antenna demonstrates monopole-like radiation characteristics.

A time-frequency plot is used to present the group delay of a UWB system, in which the time distortion from one antenna to another is described. What important it is not the value of the group delay, but its dispersion [15]. In this paper, two identical antennas were placed over a distance of 150 mm. Fig. 13 shows the group delay of the antenna system at different azimuthal angles. As shown in the figure, the variation of group time delay is less than ±0.25 ns in the UWB band, resulting in a reasonably constant group delay over the UWB band.

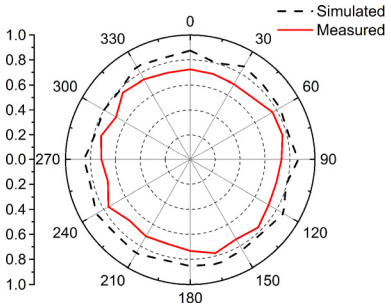

FIGURE 14. Simulated and measured System Fidelity Factor.

The System Fidelity Factor is used to quantify some type of correlation and dependence, indicating the statistical relationships between the transmission and the received pulse signals. This number quantifies the signal distortion produced by a system comprising two antennas [16]. Fig. 14 shows the simulated and measured results for the System Fidelity Factor at different azimuthal angles, which indicate that the pro-posed antenna has excellent time-domain behavior.

TABLE 2. Comparison of proposed antenna and reference antennas.

Ref	Operating frequency band (GHz)	Height (mm)	Relative height (λ_0)
[5]	2.15-14	10	0.71
[6]	0.05-2	152	0.1
[7]	0.75-2.66	15	0.08
[8]	3-11.2	10	0.1
[9]	0.9-2.4	25.4	0.068
[10]	3.06-12	8	0.08
[11]	2.8-11.4	7	0.065
[12]	3.1-10.3	10	0.08
This work	2.5-24	6	0.05

Table II shows a comparison of the characteristics of the proposed low-profile antenna with those of other designs presented in [5]–[12]. Apparently, the antenna presented in the current work has a wider impedance bandwidth and a lower profile.

IV. CONCLUSION

A low-profile UWB antenna is designed and fabricated in this work. By using a printed structure, the antenna overcomes the drawbacks of the conventional monocone antenna, such as heavyweight and difficult fabrication. The proposed antenna inherits the merits of both the monocone antenna and the printed antenna. It is light and easy to fabricate, providing

broadband and omnidirectional radiation as well. Optimized shape of the radiation patch and shorted top-loading patches are introduced to broaden bandwidth and reduce the profile of the antenna, which has a height of 0.05 λ_0. The measured and simulated results show that the antenna can achieve an enhanced impedance bandwidth of about 162% in the range of 2.5 GHz to 24 GHz ($S_{11} < -10$ dB). The results for the group delay and System Fidelity Factor indicate that the proposed antenna has satisfactory time-domain behavior in transmitting and receiving pulse signals.

REFERENCES

[1] P. S. Hall *et al.*, "Antennas and propagation for on-body communication systems," *IEEE Antennas Propag. Mag.*, vol. 49, no. 3, pp. 41–58, Jun. 2007.

[2] A. Alomainy, A. Sani, A. Rahman, J. G. Santas, and Y. Hao, "Transient characteristics of wearable antennas and radio propagation channels for ultrawideband body-centric wireless communications," *IEEE Trans. Antennas Propag.*, vol. 57, no. 4, pp. 875–884, Apr. 2009.

[3] A. Zaric, J. R. Costa, and C. A. Fernandes, "Design and ranging performance of a low-profile UWB antenna for WBAN localization applications," *IEEE Trans. Antennas Propag.*, vol. 62, no. 12, pp. 6420–6427, Dec. 2014.

[4] J. Zhao, D. Psychoudakis, C.-C. Chen, and J. L. Volakis, "Design optimization of a low-profile UWB body-of-revolution monopole antenna," *IEEE Trans. Antennas Propag.*, vol. 60, no. 12, pp. 5578–5586, Dec. 2012.

[5] H. Nakano, H. Iwaoka, K. Morishita, and J. Yamauchi, "A wideband low-profile antenna composed of a conducting body of revolution and a shorted parasitic ring," *IEEE Trans. Antennas Propag.*, vol. 56, no. 4, pp. 1187–1192, Apr. 2008.

[6] J. Zhao, T. Peng, C. C. Chen, and J. L. Volakis, "Low-profile ultrawideband inverted-hat monopole antenna for 50 MHz-2 GHz operation," *Electron. Lett.*, vol. 45, no. 3, pp. 142–144, Jan. 2009.

[7] S. L. Zuo, Y. Z. Yin, Z. Y. Zhang, and K. Song, "Enhanced bandwidth of low-profile sleeve monopole antenna for indoor base station application," *Electron. Lett.*, vol. 46, no. 24, pp. 1587–1588, Nov. 2010.

[8] N. Chahat, M. Zhadobov, R. Sauleau, and K. Ito, "A compact UWB antenna for on-body applications," *IEEE Trans. Antennas Propag.*, vol. 59, no. 4, pp. 1123–1131, Apr. 2011.

[9] D. W. Aten and R. L. Haupt, "A wideband, low profile, shorted top hat monocone antenna," *IEEE Trans. Antennas Propag.*, vol. 60, no. 10, pp. 4485–4491, Oct. 2012.

[10] M. Koohestani, J.-F. Zürcher, A. Moreira, and A. Skrivervik, "A novel, low-profile, vertically-polarized UWB antenna for WBAN," *IEEE Trans. Antennas Propag.*, vol. 62, no. 4, pp. 1888–1894, Apr. 2014.

[11] W. Jeong, J. Tak, and J. Choi, "A low-profile IR-UWB antenna with ring patch for WBAN applications," *IEEE Antennas Wireless Propag. Lett.*, vol. 14, pp. 1447–1450, 2015.

[12] M. N. Shakib, M. Moghavvemi, and W. N. L. Mahadi, "A low-profile patch antenna for ultrawideband application," *IEEE Antennas Wireless Propag. Lett.*, vol. 14, pp. 1790–1793, 2015.

[13] X. Begaud, *Ultra Wide Band Antennas*. Hoboken, NJ, USA: Wiley, 2011.

[14] W. Wiesbeck, G. Adamiuk, and C. Sturm, "Basic properties and design principles of UWB antennas," *Proc. IEEE*, vol. 97, no. 4, pp. 372–385, Feb. 2009.

[15] C. Roblin, S. Bories, and A. Sibille, "Characterization tools of antennas in the time domain," in *Proc. IWUWBS*, Oulu, Finland, Jun. 2003, pp. 1–19.

[16] G. Quintero, J. F. Zurcher, and A. K. Skrivervik, "System fidelity factor: A new method for comparing UWB antennas," *IEEE Trans. Antennas Propag.*, vol. 59, no. 4, pp. 2502–2512, Jul. 2011.

DEQIANG YANG received the B.E., M.E., and D.E. degrees from the School of Electronic Engineering, University of Electronic Science and Technology of China (UESTC), in 1992, 2006, and 2012, respectively. From 2012 to 2016, he was a Senior Engineer with UESTC. His research interests include UWB indoor localization technology, antenna measurement, and antenna theory.

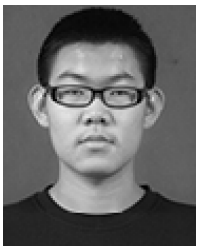

JIANZHONG HU received the B.E. degree from the School of Electronic Engineering, University of Electronic Science and Technology of China (UESTC), in 2016, where he is currently pursuing the M.E. degree. His research interests include UWB antenna, microwave power transmission, and EMC technology.

SIHAO LIU received the B.E. and M.E. degrees from the School of Electronic Engineering, University of Electronic Science and Technology of China (UESTC), in 2013 and 2016, respectively, where he is currently pursuing the Ph.D. degree. His research interests include UWB antenna, microwave power transmission, and MIMO technology.